NASA TECHNICAL MEMORANDUM

NASA TM X-71710

NASA TM X-71710

(NASA-TM-X-71710) ANELASTIC DEFORMATION OF BORON FIBERS (NASA) 16 p HC $3.25 CSCL 11D

N75-23697

Unclas

G3/24 21848

ANELASTIC DEFORMATION OF BORON FIBERS

by James A. DiCarlo
Lewis Research Center
Cleveland, Ohio 44135

TECHNICAL PAPER presented at
American Physical Society Meeting
Denver, Colorado, March 31 - April 3, 1975

E-8326

ANELASTIC DEFORMATION OF BORON FIBERS

by James A. DiCarlo

Lewis Research Center
National Aeronautics and Space Administration
Cleveland, Ohio

SUMMARY

The flexural deformation behavior of vapor-deposited boron fibers was examined from 100° to 1100° K by stress-relaxation and internal friction techniques. Only strong thermally-activated anelasticity was observed with no evidence of plasticity up to surface strains of 6×10^{-3}. The parameters governing the relaxation processes within the anelastic spectra of as-received and annealed fibers were determined. These parameters were correlated with X-ray structure studies to develop preliminary models for the sources of boron's anelasticity. The large relaxation strengths of the dominant Ia processes coupled with their relaxation times and energies suggest a sliding mechanism between certain basic structural subunits common to both the β-rhombohedral and vapor-deposited boron structures.

INTRODUCTION

Vapor-deposited boron fibers employed as strengthening elements in advanced composites are generally produced by the hydrogen reduction of BCl_3 on a 13 μm tungsten filament held at temperatures near 1300° C (Ref. 1). The structure of the deposited boron is usually considered amorphous because its powder X-ray spectrum consists of only a few diffuse halos. A schematic longitudinal section of the amorphous fiber given in Fig. 1 shows the tungsten substrate and the residual stress pattern which exists within the boron after deposition and quenching. This pattern, which also exists in the hoop direction, varies monotonically from tension near the core to over 100 ksi compression at the surface. It is this compressive surface state which gives the boron fiber its surface flaw insensitivity and high strength and makes it ideally suited for composites.

Besides high strength, boron fibers display an unusually high degree of anelasticity. For example, bending a fiber to radius R_0 (Fig. 1), raising the temperature to T, holding for time t, and then quenching to room temperature, results in a bent fiber with radius R when the initial strain is removed. Reheating the fiber under zero strain returns it to its original straight condition, indicating that the deformation is totally anelastic with <u>no</u> plastic component (complete recoverability).

The purpose of this report is to describe some of our initial results concerning the characteristics and mechanisms responsible for boron's anelasticity. The principal specimens employed were 203 μm (8 mil) diameter fibers commercially produced by Avco Systems Division. Purity of the deposited boron was estimated to be greater than 99%. Flexural stress-relaxation and internal friction techniques were employed to simplify the experimental measurements and to eliminate any effects of the 16 μm borided tungsten core. Supporting structural information was obtained with powder camera X-ray data on whole fibers.

PROCEDURE AND RESULTS

Stress-Relaxation

Flexural stress-relaxation measurements (FSR) were performed (Fig. 2) in which the stress ratio m was determined as a function of temperature at a constant time of 1.0 hour. Under the assumption that the fibers display complete anelasticity (Ref. 2), the m ratio is independent of applied strain and thus of position in the flexed fiber. It is therefore calculable from the relation

$$m(T,t) = \varepsilon_e(T,t)/\varepsilon_e(T,0) = 1 - \varepsilon_a(T,t)/\varepsilon_o \tag{1}$$

where ε_e, ε_o, and ε_a are, respectively, the elastic, total, and anelastic strain at any point within the fiber. The values of ε_a were measured from the deformation remaining in the fiber after annealing for time t at temperature T, quenching, and removing the applied strain ε_o.

Curve a of Fig. 2 was obtained with a cantilevered specimen configuration. Because the strain at any point is proportional to the end displacement X, Eq. (1) simplifies to

$$m(T,t) = 1 - X_a(T,t)/X_o \tag{2a}$$

The use of this relation is justified by the fact that the m data of curve a were found to be strain-independent for the indicated range of average surface strain $\overline{\varepsilon}_s$. These results were also found to be independent of fiber diameter down to 102 μm (4 mil). The strong anelasticity of the fiber is clearly evident. In fact, from the tensile creep data of Ellison and Boone (Ref. 3), it is estimated that the stress ratio will reach values as low as 25%.

Curve b of Fig. 2 was obtained by retaining the fiber in a constant radius configuration within a stainless steel tube of 3.5 cm inside diameter. Here strain at any point is inversely proportional to radius of curvature R so that

$$m(T,t) = 1 - R_o/R_a(T,t) \tag{2b}$$

Comparing curves a and b, one finds that if the strain is high enough, boron's stress ratio becomes strain-dependent. Thus, at some surface strain level above 10^{-3}, the anelastic requirement of a unique relation between anelastic strain and applied stress measurably breaks down. This occurs even though the fibers of curve b do display the property of complete recoverability. Finally, the common point at $m = 0.57$ remains unexplained, except perhaps that this m value corresponds quite well with the Zener relaxation strength (Ref. 4) expected for crystallite sliding and boron's Poisson's ratio of 0.21 (Ref. 5).

Internal Friction

From the FSR behavior it is clear that the processes controlling boron's anelasticity possess thermally-activated relaxation times τ governed by the Arrhenius equation:

$$\tau = \tau_o \exp(Q/kT) \tag{3}$$

The characteristic parameters τ_o and Q are, respectively, the infinite T relaxation time and the relaxation energy. To determine these parameters for each process within the boron fibers, we have supplemented the FSR data with flexural internal friction data taken at the fundamental and first overtone resonant modes of a vibrating cantilevered specimen (Ref. 6). The frequency (f) range 10^2 to 10^4 Hz was examined with specimen lengths between 1 and 6 cm (boron modulus = 38×10^{11} dynes/cm^2). Friction maxima occurred when $f = (2\pi\tau)^{-1}$. For fibers clamped between stainless steel plates, the background friction of the total system was estimated to be less than 10^{-4} (log decrement).

The high temperature internal friction of a typical amorphous boron fiber (8 mil) shows a large peak which shifts in temperature with frequency (Fig. 3). During the initial warmup of all as-received fibers, a slight drop in friction amounting to $\sim10^{-3}$ was observed between 100° and 400° C. This annealing effect is attributed to some unknown imperfection which probably exists in the boron because of the rapid quench during production. The Fig. 3 results indicate the stable friction spectra observed after this initial warmup behavior. All friction data were strain-independent for strains from 10^{-6} to 10^{-4} and were reproducible to within 10% from specimen to specimen. Regarding relaxation parameters, the low temperature side of the amorphous peak was best combined with the low strain FSR data by assuming a constant relaxation time τ_o and a broad Gaussian distribution in controlling energy (Ref. 2). By so doing, the two Fig. 3 peaks labeled Ia and Ib were revealed for the amorphous boron.

In order to determine the effects of structure on anelasticity, amorphous fibers were annealed at 1300°, 1500°, and 1700° C for 1 hour at 10^{-7} mm Hg. On the larger scale of Fig. 4 we again show the amorphous peaks Ia and Ib. By annealing at 1300° or 1500° C these peaks disappear, leaving primarily a new lower temperature peak Ia* which is in turn replaced by another peak Ia** when the anneal is taken to 1700° C. The application of a Gaussian distribution in energy to the three Ia peaks shows that the temperature shift is caused solely by a lowering of the average energy. For Ia**, however, a large increase in relaxation strength is observed. Powder camera X-ray data on the annealed fibers show that the only effect of the 1300° C anneal is to add the lines of boron's β-rhombohedral polymorph to the already existing amorphous halo spectrum. At 1700° C the amorphous halos disappear, leaving only the β lines.

All relaxation parameter results are summarized in Table I. Here the relaxation strength Δ is defined as the total change in stress ratio m if complete relaxation of the process were observed without the influence of preceeding processes (Ref. 2). Q_p is the center Gaussian energy and β_Q measures one-half the Gaussian width at e^{-1} maximum. The Ia and Ib processes contribute about the first 25% of the Fig. 2 stress relaxation, leaving about another 50% to be accounted for. These remaining processes are grouped under the label II. Their average parameters were estimated from limited tensile creep data in the literature (Ref. 7). It is seen that the II characteristic times are quite long. Finally, Table I also includes the derived parameters for two low temperature boron peaks, A and B, shown in Fig. 5.

DISCUSSION

Because of the complexity of boron's morphology (Ref. 8), it would be difficult at the present time to arrive at definitive conclusions concerning the sources of the anelastic spectra of this study. There are, however, some interesting preliminary models which can be developed by examining the results of Table I in the light of anelastic theory and existing data on the structure of amorphous and crystalline boron. For purposes of discussion and consistency with the boron literature, the as-received vapor-deposited fibers will be considered amorphous even though the meaning of this term varies with one's particular point of view.

Ia Relaxation

Proper discussion of the dominant Ia peaks should begin above 1300° C where the structural ground is the firmest. From the X-ray data on the annealed fibers, it follows that peaks Ia* and Ia** should be assigned to crystalline processes within the β-rhombohedral structure. Regarding a possible mechanism for the β process, the magnitude of the Ia** relaxation strength is comparable to that predicted by Zener for grain boundary sliding ($\Delta = 43\%$), thereby suggesting a mechanism of equal or similar nature. That is, the large strength would seem to require a model in which the 1700° C fiber is composed almost enirely of the Ia** relaxing entity, be it β boron crystallites or grains or some smaller β subunit. It follows that the increase in relaxation strength from 1300° to 1700° C can be interpreted as an approximate doubling of the fiber volume containing the β process. The coupling of this interpretation with the Fig. 4 data further suggests that the amorphous structure retained between 1300° and 1700° C cannot support the Ia process to the same degree as the original as-received structure.

The τ_0 and Δ values for the amorphous peak Ia suggest a relaxation mechanism similar to that of Ia*; crystallite sliding, for example. The difference in Q and β_Q could then be attributed to the lattice environment change from a highly-defected amorphous structure to the better ordered β boron structure. Significantly, the existence of an anelastic effect with a fairly well-defined energy is indeed an indication of some degree of crystallinity within the vapor-deposited fibers. The constancy of the Ia relaxation strength up to 1500° C suggests that the β morphology already exists in the amorphous fibers. The fact, however, that X-ray data on these fibers do not show the high-intensity d spacings of the β-rhombohedral structure has been employed by Lindquist et al. to argue against this point of view (Ref. 9). Gillespie, on the other hand, employs the fairly strong β lines which fall within the amorphous halos to suggest the vapor-deposited fibers may contain microcrystalline deposits of β boron (Ref. 10). In the preliminary stages of the present work, this author also felt that the Ia process could be explained by a β morphology model (Ref. 11). In the interest of developing a fuller understanding of the anelastic results, we shall briefly discuss this model.

Assuming the β process is operating within each peak, one might attribute the energy difference between Ia and Ia* to a stress-dependent Q which is higher under the residual compressive surface state present in the vapor-deposited fibers (Fig. 1). The flexural measurements, being sensitive to only surface relaxations, should then yield a Q_p (1.7 eV) which is larger than the Q_p at zero stress (1.4 eV). It could be assumed further that above 1300° C the residual stress pattern disappears, allowing all β processes to relax at the zero-stress energy. This model is also supported by the strain dependence of FSR and tensile creep (Ref. 12) which could be interpreted as a tensile lowering of the anelastic energy. The validity of this model appears to be negated, however, by recent theoretical and experimental evidence. First, the ratio of the change in Q_p to the maximum residual surface strain (Ref. 13) corresponds to values of the order of magnitude of 100 eV, which is much higher than one would expect for typical solid state processes. Second, since the surface contains the highest residual strain, the derived energy distribution should be weighted toward high energies and thus should not be Gaussian. Finally, preliminary results on the fiber etched down to a 135 μm diameter show no change in the relaxation spectrum, although a large decrease in surface strain is observed (Ref. 13).

The above evidence argues against a significant role for residual stress in the Q_p values, but still does not disallow the existence of β boron within the amorphous fibers. How then does one explain the absent β X-ray lines? Perhaps a possible answer lies in a more thorough consideration of the proposed model of crystallite sliding. Typical metallic grain-boundary sliding or relaxation is controlled by a Q which can be equated to the material's energy for self-diffusion, be it within the bulk or along the grains (Ref. 2). For this reason the observation of internal friction peaks due to the boundary mechanism requires frequencies in the subsonic range to avoid recrystallization effects. Basically these effects increase the diameter of the grains, thereby increasing the τ_o of the relaxation and pushing the peak to higher temperatures during observation. Operating at the audio frequencies of this study, one should not expect to cover the whole grain boundary peak without finding some irreversible friction changes upon cooling. Clearly the results of Fig. 4 and the temperatures required for morphology changes indicate that the Ia processes do not show any recrystallization effects. This fact is also supported by the commonly employed empirical relation for metallic bulk self-diffusion energy: $Q \cong 18\ kT_m$. This relation yields an energy for boron (∿3.6 eV) much different than $Q_p = 1.4$ eV.

The arguments against crystallite sliding by atomic diffusion are of course weakened by a lack of theoretical and experimental data on imperfection motion in covalent boron. Assuming the validity of these arguments, one may still retain the sliding model by considering the relaxation to occur not by atomic diffusion between large crystallites but by the breaking of atomic bonds between smaller subunits in the boron structure. These basic subunits are contained in both the vapor-deposited and β-rhombohedral structures and thus can anelastically relax within both forms. The 1300° C anneal does not alter the density of subunits but merely changes their lattice environment from short-range order with broad distribution of short bond lengths (Q = 1.7 eV) to long-range β crystalline order with a narrower distribution of longer bond lengths (Q = 1.4 eV). Experimentally the magnitude and constancy of τ_o support such a model. Also, it is well known theoretically that the boron polymorphs do contain subunits larger than single atoms (Refs. 8 and 14). For example, there is the basic 12 atom B_{12} icosahedron, which is common to all boron forms, and the more complicated 84 atom B_{84} truncated icosahedron which comprises the β-tetragonal and β-rhombohedral polymorphs.

Certainly the above model for the Ia processes is only tentative at the present time. A more definitive mechanism requires additional data and theory, such as, structural and impurity analyses of each fiber type, anelastic measurements on single and polycrystalline boron polymorphs, and a basic understanding of diffusion and possible imperfections within the different structures. Also to be considered is an apparent correlation between anelastic and electronic energies of semiconducting boron. For example, the Q_p of 1.39 eV for the β-rhombohedral Ia** peak is in excellent agreement with this polymorph's band gap as determined by the temperature dependence of electrical conductivity (Ref. 15). This agreement may be coincidental, but optical absorption and reflectivity data taken on amorphous boron film (Ref. 16) suggest that this material possesses a broad distribution in gap energy centered near 1.7 eV. In addition, the Q for the low temperature B peak correlates well with the energy of the highly dense electron trap in β boron (Ref. 17). Finally, for α-tetragonal and α-rhombohedral, the two polymorphs considered to best explain the d spacings and density of amorphous boron (Ref. 9), one finds gap energies above 1.6 eV as evidenced by measurement (Ref. 18) and their ability to transmit red light (Ref. 8). Only further work will establish the validity of this anelastic/electronic correlation and its possible inclusion in a more detailed model for boron anelasticity. Obviously such a correlation would fit well into the boron subunit relaxation mechanism.

Other Relaxations

The structural X-ray results on annealed fibers suggest that the Ib relaxation process is only active when the boron displays an amorphous halo spectrum. From the strength data of Table I it appears that near 1300° C approximately half of the Ib mechanism is lost in creation of the Ia* process. The remaining half is lost near 1700° C when the β process approximately doubles to maximum strength. This strength behavior supports a crystallite sliding mechanism for Ib also. The τ_o value, however, points to relaxing entities larger than those relaxing in the Ia processes. It also indicates a possible structural relationship with the low temperature A peak. These correlations of relaxation parameters are indeed interesting and should be very useful for developing structural models of amorphous fibers.

For a description of the engineering creep behavior of vapor-deposited fibers, relaxation process II and its parameters are certainly the most important. However, because the II internal friction behavior is not observable below 800° C at the audio frequencies of this study, it's relaxation characteristics are not accurate enough for a fundamental interpretation. In fact, it is very probable that the II relaxation strength is produced by more than one process and that the Table I data represent average parameters. Based on the trend set by processes Ia and Ib, one might envision a series of mechanisms with the approximately same Q_p but with increasing values of τ_0. For a sliding mechanism this τ_0 trend would imply larger and larger crystallites. Perhaps the common m point in Fig. 2 indicates the end of one type of mechanism and the beginning of another. This latter process may be related to grain-boundary relaxation by atomic diffusion. Obviously more process II data and theory is required, especially on the annealed fibers.

CONCLUDING REMARKS

The anelastic results of this initial study have many practical and fundamental implications. On the applied side, one can now predict with a fair degree of accuracy the time-dependent flexural deformation of vapor-deposited boron fibers in the temperature and stress range of expected use in advanced composites. These predictions can be applied directly to such fiber/composite properties as creep, modulus, damping capacity, formability, and impact strength. The conclusion that the residual stress pattern plays little part in the anelastic response suggests that the data is not limited to flexural properties but applies also to tensile and torsional behavior. In addition, the quite dramatic change in internal friction brought on by fiber crystallization (Fig. 4) indicates a possible nondestructive technique for evaluating composite strength degradation brought on by matrix-induced structural changes in the amorphous fibers. It should also be emphasized that all measurements of this work were done in vacuums of less than 10^{-4} mm Hg. Preliminary results on amorphous fibers heated in air show measurable decreases in internal friction, thereby suggesting the additional capability for detecting environmental contamination.

On the basic side, the discussion of relaxation parameters revealed many interesting possible relationships between anelastic response, atomic structure, and electronic properties of boron. Further anelastic-structural measurements should provide a clearer picture of the amorphous structure and its relationship with the β-rhombohedral structure. The introduction of electronic energies into this picture will take on added fundamental significance since as yet there is no model to explain boron's electronic behavior on a structural basis. Perhaps the present finding of a crystallite sliding energy which is apparently related to the band gap energy and not the normal self-diffusion energy will aid in developing such a model.

REFERENCES

1. Line, Lloyd E., Jr.; and Henderson, U. V., Jr.: Boron Filament and Other Reinforcements Produced by Chemical Vapor Plating. Handbook of Fiberglass and Advanced Plastics Composites, George Lubin, ed., Van Nostrand Reinhold, 1969, pp. 201-236.

2. Nowick, A. S.; and Berry, B. S.: Anelastic Relaxation in Crystalline Solids. Academic Press, 1972.

3. Ellison, E. G.; and Boone, D. H.: Some Mechanical Properties of Boron-Tungsten Boride Filaments. J. Less-Com Metals, vol. 13, 1967, pp. 103-111.

4. Zener, Clarence: Theory of the Elasticity of Polycrystals with Viscous Grain Boundaries. Phys. Rev., vol. 60, Dec. 1941, pp. 906-908.

5. Wawner, Franklin E., Jr.: Boron Filaments. Modern Composite Materials, Laurence Broutman and R. Krock, eds., Addison-Wesley, 1967, pp. 244-269.

6. DiCarlo, J. A.; Snead, C. L., Jr.; and Goland, A. N.: Stage-I Interstitials in Electron-Irradiated Tungsten. Phys. Rev., vol. 178, no. 3, Feb. 1969, pp. 1059-1072.

7. Antony, K. C.; and Chang, W. H.: Mechanical Properties of Al-B Composites. Trans. Am. Soc. Metals, vol. 61, no. 3, Sept. 1968, pp. 550-558.

8. Newkirk, A. E.: Elemental Boron. Boron, Metallo-Boron Compounds, and Boranes, Roy M. Adams, ed., Interscience, 1964, pp. 233-299.

9. Lindquist, P. F.; Hammond, M. L.; and Bragg, R. H.: Crystal Structure of Vapor-Deposited Boron Filaments. J. Appl. Phys., vol. 39, no. 11, Oct. 1968, pp. 5152-5162.

10. Gillespie, J. S., Jr: Crystallization of Massive Amorphous Boron. J. Am. Chem. Soc., vol. 88, no. 11, June 1966, pp. 2423-2425.

11. DiCarlo, J. A.: Anelastic Deformation of Boron Fibers. Abstract FL 18, Bull. Am. Phys. Soc., vol. 20, no. 3, 1975, p. 446.

12. Ericksen, R. H.: Room Temperature Creep of Borsic-Aluminum Composites. Met. Trans., vol. 4, 1973, pp. 1687-1693.

13. Behrendt, D. R.: Private communication, NASA Lewis Research Center.

14. Matkovich, V. I.; Giese, R. F., Jr.; and Economy, J.: Packing of B_{12} Groups in Boron and Boride Structures. Z. Krist., vol. 122, 1965, pp. 116-130.

15. Gaule, Gerhart K., ed: Boron. Vol. II, Plenum Press, 1965.

16. Feldman, Charles; Ordway, Fred; and Zimmerman, William, III: Vacuum-Deposited Amorphous Boron Films. Boron, Vol. II, Gerhart K. Gaule, ed., Plenum Press, 1965, pp. 235-260.

17. Werheit, H.: Optical and Photoelectrical Properties of β-Rhombohedral Boron. Phys. Stat. Sol., vol. 39, no. 1, 1970, pp. 109-120.

18. Horn, F. H.: Some Electrical and Optical Properties of Simple Rhombohedral Boron. J. Appl. Phys., vol. 30, no. 10, Oct. 1959, pp. 1611-1612.

TABLE I. - ANELASTIC RELAXATION PARAMETERS OF VAPOR-DEPOSITED AND ANNEALED BORON FIBERS

Relaxation process	Onset, T, °C	$\log \tau_0$	Δ, %	Q_p, eV	β_Q, eV
High temperature					
Ia	<400	-14.0∓0.5	16±2	1.72±0.08	0.31±0.03
Ia*	1300	-14.8∓0.4	17±1	1.46±0.05	0.15±0.02
Ia**	1700	-14.4∓0.2	35±3	1.39±0.03	0.15±0.02
Ib	<400	-11.2∓0.2	7±1	1.68±0.09	0.17±0.03
Ib*	1300	---------	<4	---------	---------
Ib**	1700	---------	∼0	---------	---------
II	<400	3±3	∼70	0.45±0.1	---------
Low temperature					
A	As-rec	-10∓1	0.3±0.1	0.10±0.02	---------
A*/**	1300	---------	∼0	---------	---------
B	As-rec	---------	>0	---------	---------
B*/**	1300	-14.3∓1.2	0.3±0.1	0.46±0.06	---------

FIGURE CAPTIONS

1. Schematic representations of the residual stress pattern and anelastic deformation behavior of vapor-deposited boron fibers.
2. The flexural stress relaxation characteristics of vapor-deposited boron fibers as a function of temperature and strain at a constant time of 1.0 hr.
3. The internal friction of vapor-deposited boron fibers after one hour at 400 C. Peaks Ia and Ib are derived from different τ_0, and gaussian distributions in energy with approximately the same Q_p.
4. The effects of one hour anneals at 1300 and 1700 C on the high temperature internal friction of vapor-deposited boron fibers.
5. The effects of one hour anneals at 400 and 1300 - 1700 C on the low temperature internal friction of vapor-deposited boron fibers.

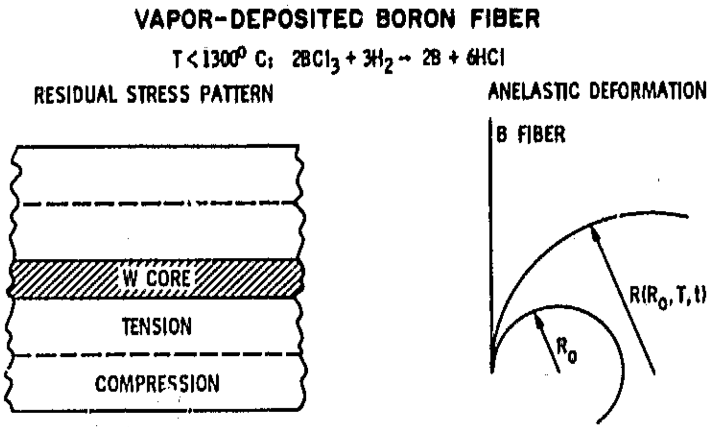

Figure 1

E-8326

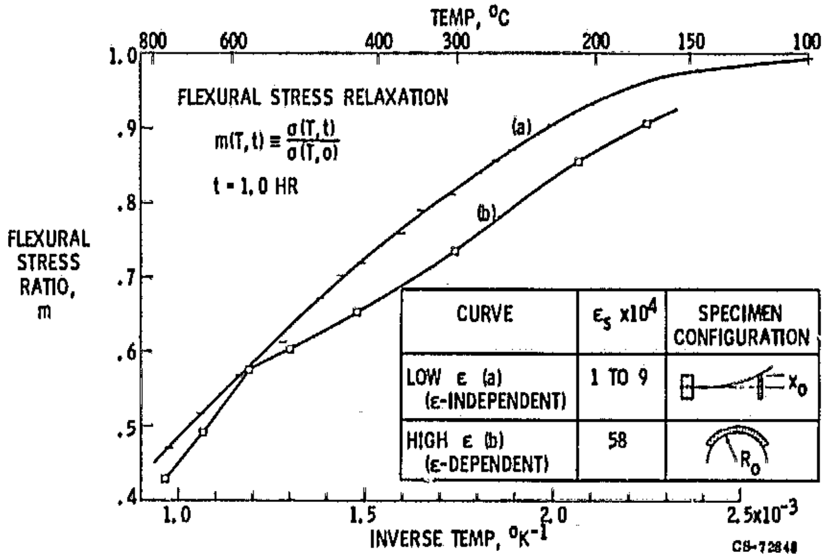

Figure 2

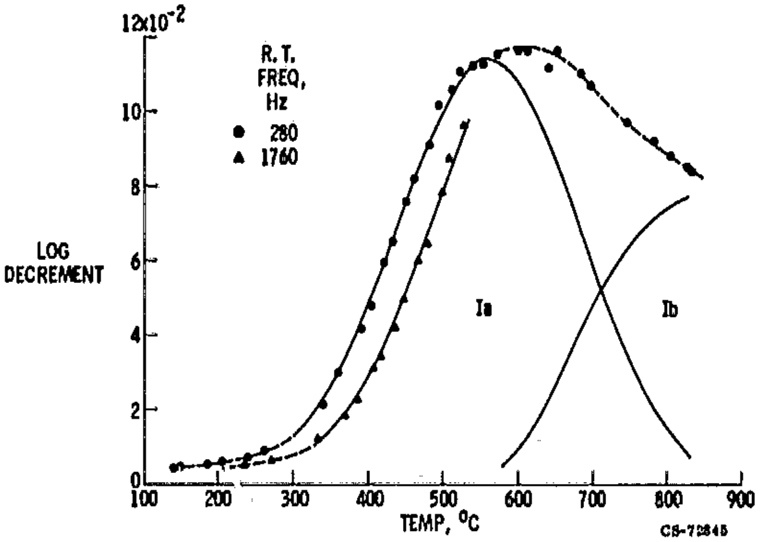

Figure 3

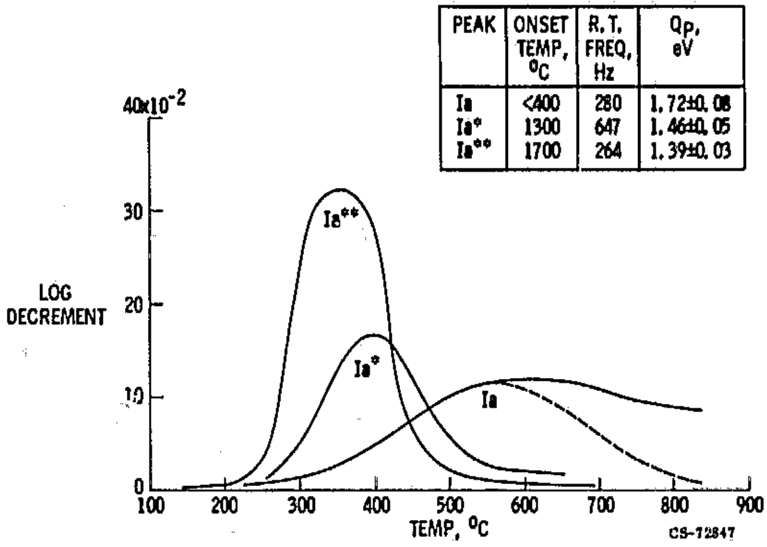

PEAK	ONSET TEMP, °C	R. T. FREQ, Hz	Qp, eV
Ia	<400	280	1.72±0.08
Ia*	1300	647	1.46±0.05
Ia**	1700	264	1.39±0.03

Figure 4

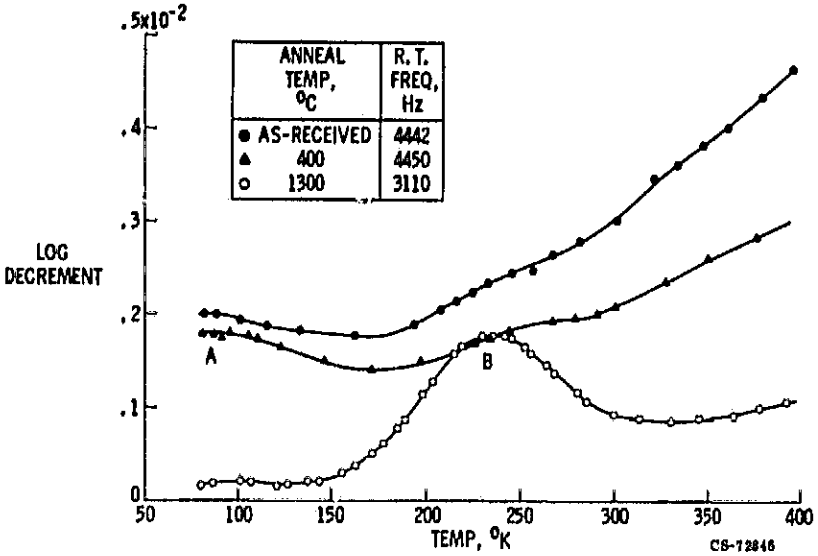

Figure 5

E-8326

NASA-Lewis